Heat Transport in the Geostrophic Regime of Rotating Rayleigh-Bénard Convection

Robert E. Ecke[1,*] and Joseph J. Niemela[2]

[1]Center for Nonlinear Studies, Los Alamos National Laboratory, Los Alamos, New Mexico 87545, USA

[2]International Centre for Theoretical Physics, Strada Costiera 11, 34014 Trieste, Italy

(Received 19 August 2013; revised manuscript received 25 April 2014; published 8 September 2014)

We report experimental measurements of heat transport in rotating Rayleigh-Bénard convection in a cylindrical convection cell with an aspect ratio of $\Gamma = 1/2$. The fluid is helium gas with a Prandtl number $\mathrm{Pr} = 0.7$. The range of control parameters for Rayleigh numbers $4 \times 10^9 < \mathrm{Ra} < 4 \times 10^{11}$ and for Ekman numbers $2 \times 10^{-7} < \mathrm{Ek} < 3 \times 10^{-5}$ (corresponding to Taylor numbers $4 \times 10^9 < \mathrm{Ta} < 1 \times 10^{14}$ and convective Rossby numbers $0.07 < \mathrm{Ro} < 5$). We determine the transition from weakly rotating turbulent convection to rotation dominated geostrophic convection through experimental measurements of the heat transport Nu. The heat transport, best collapsed using a parameter RaEk^β with $1.65 < \beta < 1.8$, defines two boundaries in the phase diagram of $\mathrm{Ra}/\mathrm{Ra}_c$ versus Ek and elucidates properties of the geostrophic turbulence regime of rotating thermal convection. We find $\mathrm{Nu} \sim (\mathrm{Ra}/\mathrm{Ra}_c)^\gamma$ with $\gamma \approx 1$ from direct measurement and $1.2 < \gamma < 1.6$ inferred from scaling arguments.

DOI: 10.1103/PhysRevLett.113.114301 PACS numbers: 44.25.+f, 47.27.-i, 47.32.-y, 47.55.pb

Thermal convection in the presence of rotation occurs in many geophysical contexts, including Earth's outer core [1], oceans [2], planetary atmospheres such as Jupiter [3], and solar interiors [4]. In these geophysical systems the form of the convective state and the resulting heat transport are far beyond direct numerical computation or inaccessible to direct measurement, having dimensionless parameters characterizing rotation and buoyancy of order $\mathrm{Ek} \sim 10^{-15}$ and $\mathrm{Ra} \sim 10^{20}$. The boundaries between very different regimes of heat transport depend on the combination of these parameters so determining their relationships is critical for understanding how heat is transported in important geophysical contexts. Laboratory experiments [5–13] that balance rotation and buoyancy in a controlled environment and that allow for precise measurements provide an important approach to understanding and predicting heat transport scaling for rotating convection. Theoretical [14,15] and numerical simulations [16–18] complement the laboratory experiments, making the problem of rotating thermal convection of interest across a wide spectrum of scientific disciplines from fundamental fluid dynamics to natural systems including planetary and solar atmospheres.

The parameters of rotating convection for a layer of fluid heated from below and rotated about a vertical axis are the Rayleigh number $\mathrm{Ra} = g\alpha\Delta T d^3/\nu\kappa$ which measures the buoyant forcing of the flow, the Ekman number $\mathrm{Ek} = \nu/(2d^2\Omega)$ which represents an inverse dimensionless rotation rate, and the Prandtl number $\mathrm{Pr} = \nu/\kappa$. In these definitions g is the acceleration of gravity, ΔT is the temperature difference between top and bottom plates separated by a distance d, ν and κ are the fluid kinematic viscosity and thermal diffusivity, respectively, and Ω is the angular rotation frequency. Rotation can also be represented by the Taylor number $\mathrm{Ta} = \mathrm{Ek}^{-2}$ or by the convective Rossby number $\mathrm{Ro} = \mathrm{Ek}\sqrt{\mathrm{Ra}/\mathrm{Pr}}$ which reflects the ratio of rotational time to buoyancy time. Here we use the representation of Ek or Ro such that high dimensionless rotation rates correspond to small values of the rotational control parameter in the spirit of the asymptotic equation approach of expanding in a small variable [17]. The measured response of the system in this space of buoyant and rotational forcing is the Nusselt number, $\mathrm{Nu} = \dot{Q}/(\lambda\Delta T)$ where $\dot{Q}$ is the applied heater power through the fluid and λ is the thermal conductance of the fluid.

Much of the experimental work on rotating convection at high dimensionless rotation rates has focused on either the transition to convection where rotation-induced wall modes play an important role [6,19,20] or the turbulent state far from onset where thermal boundary layers control heat transport [5,7–10]. Recently, the numerical simulation [21,22] of asymptotic equations of motion [17] in the limit of high rotation rate has focused on heat transport above the convective onset but below the transition to nonrotational boundary-layer controlled turbulence—a region they refer to as the geostrophic regime where the local balance of Coriolis force and pressure in the bulk dominates at large scales (to order Ro) and restricts the form of convective structures (where most vertical transport happens) to smaller and smaller lateral spatial scales. These equations need experimental validation in order to serve as an extrapolation for much higher effective rotation rates. In particular, predictions have been made for the power-law dependence of Nu on Ra in the geostrophic range: $\mathrm{Ra}^{3/2}$ based on numerical simulations of asymptotic equations [22] and Ra^3 based on dimensional boundary layer arguments [23,24]. The data in this regime are scarce and the explored range of Pr, Ek, and Ra is very limited. In particular, the crossovers from buoyancy dominated turbulent convection (where rotation has no measurable effect) to rotation-influenced turbulent convection (dominated by thermal boundary layer development) to geostrophic turbulence (Ek small) have not been well investigated. Thus, extrapolation of results of laboratory experiments and numerical simulations to important geophysical systems remains uncertain.

The experimental apparatus used for these studies was described in detail previously [25,26]. The convection cell had a cylindrical geometry with height $d = 100$ cm and diameter 50 cm resulting in an aspect ratio $\Gamma = 1/2$. The working fluid was helium gas near its critical point at around 5.2 K, and the range of Ra and Ek was controlled by varying ΔT in the range 0.04–0.30 K at a mean cell temperature between 4.61 and 4.75 K and using densities ρ of 0.000 33, 0.000 66, 0.0013, and 0.0018 g/cc. For these values of ρ and ΔT, $\mathrm{Pr} = 0.7$. For most of the runs, the rotation rate f ($\Omega = 2\pi f$) was fixed at the maximum for the apparatus corresponding to 0.167 Hz resulting in runs at constant Ek (and Ta). In one run, Ra was fixed and f varied between 0.0056 and 0.167 Hz. For all the data, Nu was measured without rotation as a reference and is denoted $\mathrm{Nu}_0 = 0.121\mathrm{Ra}^{0.307}$ [25]. The data are reported in ratios of $\mathrm{Nu}(\mathrm{Ra}, \Omega)/\mathrm{Nu}_0(\mathrm{Ra}, 0)$ that to first order compensate for small systematic uncertainties and facilitate comparison to other data sets.

We measure the convective heat transport Nu and explore the crossover from rotation-influenced turbulent convection to geostrophic rotating turbulence over a parameter range $2 \times 10^{-7} < \mathrm{Ek} < 3 \times 10^{-5}$ and $4 \times 10^9 < \mathrm{Ra} < 4 \times 10^{11}$, corresponding to a range of convective Rossby Number, $0.07 < \mathrm{Ro} < 5$. Our work extends the experimentally measured range of Ek by about 1.5 decades (3 decades in Ta) compared to previous experimental work [5–13]. We find that the crossover from buoyancy dominated turbulence to rotation-influenced turbulent convection has a strong Pr dependence, occurring at $\mathrm{Ro}_T \approx 2$ for $\mathrm{Pr} \approx 6$ compared to $\mathrm{Ro}_T \approx 0.3$ for $\mathrm{Pr} = 0.7$ (constant Ro_T corresponds to $\mathrm{Ra}_T = \mathrm{Pr}\mathrm{Ro}_T^2\mathrm{Ek}^{-2}$). The crossover from rotation-influenced turbulent convection to geostrophic turbulence, denoted by subscript t, has a much weaker dependence on Pr but a power-law dependence on Ek that appears to steepen with decreasing Ek. The best fit to our experimental data yields $\mathrm{Ra}_t = 0.25\mathrm{Ek}^{-\beta}$ with $\beta = 1.8 \pm 0.08$ whereas data at higher Ek are consistent with a somewhat lower power [8,24], i.e., $\beta \approx 1.65 \pm 0.1$. Finally, we find that the power-law dependence of Nu with Ra in the geostrophic regime is consistent with a power law of order 1; no evidence for power-law scaling of $\mathrm{Nu} \sim \mathrm{Ra}^3$ [24] is found. Our results elucidate the accessibility of the geostrophic regime and the dependencies of Nu on Ra and Ek within it.

As in earlier experiments [25] in this apparatus at much higher Ra and $\mathrm{Pr} = 6$, $\mathrm{Nu}/\mathrm{Nu}_0 \leq 1$ for all parameters measured as shown in Fig. 1. The data are for four different runs corresponding to constant Ek between 10^{-6} and 10^{-7} and for one run at constant $\mathrm{Ra} = 6.2 \times 10^9$ (the slight

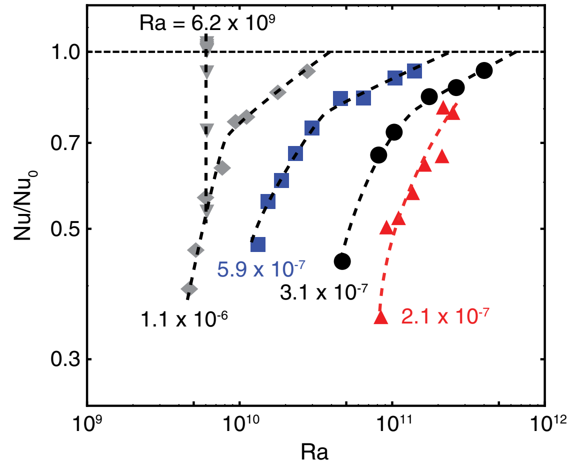

FIG. 1 (color online). $\mathrm{Nu}/\mathrm{Nu}_0$ vs Ra for constant Ek: 1.1×10^{-6} (solid diamond, gray), 5.9×10^{-7} (solid square, blue), 3.1×10^{-7} (solid circle, black), 2.1×10^{-7} (solid up triangle, red), and for constant $\mathrm{Ra} = 6.2 \times 10^9$ (solid down triangle, gray). Dashed lines are guides to the eye.

increase of $\mathrm{Nu}/\mathrm{Nu}_0 > 1$ for the run at constant Ra may be significant). From these data, we determine the Ek-dependent values of Ra_T where $\mathrm{Nu}/\mathrm{Nu}_0$ drops below 1. These transition values have an Ek dependence described well by $\mathrm{Ra}_T \sim \mathrm{Ek}^{-2}$ consistent with a constant $\mathrm{Ro} \approx 0.35$. The data also suggest a second change in slope of the curves for smaller Ra but this behavior shows up more clearly if we scale the data so that they collapse onto a single curve.

One possibility for collapsing the data is to plot them in terms of Ro (proportional to $\mathrm{Ra}^{1/2}\mathrm{Ek}$) which we show in Fig. 2. The collapse is reasonable although the simulation data [9] at much lower Ra are not captured well. The collapse does suggest two ranges of behavior consisting of an initial decrease in $\mathrm{Nu}/\mathrm{Nu}_0$ with decreasing Ro starting at $\mathrm{Ro}_T \approx 0.35$ and a second more rapid decrease starting at $\mathrm{Ro}_t \approx 0.1$. $\mathrm{Nu}/\mathrm{Nu}_0$ has dropped to about 0.8 at this second decrease. The solid lines indicate power law curves corresponding to $\mathrm{Nu} \sim \mathrm{Ra}^{0.45}$ for the first decrease and $\mathrm{Nu} \sim \mathrm{Ra}^{1.1}$ for the faster decrease. No strong conclusions can be drawn from these relationships given their short range; we revisit this below. The lack of collapse of the simulation data at much lower Ra, however, anticipates that the scaling might be improved.

Recently, measurements in water with $\mathrm{Pr} \approx 6$ were conducted [8] in which the crossover between the boundary-layer dominated turbulent state and geostrophic turbulent convection with $\mathrm{Nu}/\mathrm{Nu}_0 < 1$ was attributed to competing thermal and Ekman boundary layers. The resulting empirical crossover was found to have the form $\mathrm{Ra}_t = 1.4\mathrm{Ek}^{-7/4}$, suggesting the scaling variable $\mathrm{Ra}\,\mathrm{Ek}^{7/4}$. We show the data normalized in this manner in Fig. 3. The collapse for our data is better for this relationship and the simulation data are now collapsed as well. Using the exponent of Ek as an adjustable parameter, i.e., $\mathrm{Ra}\,\mathrm{Ek}^{\beta}$ yields $\beta = 1.8 \pm 0.1$

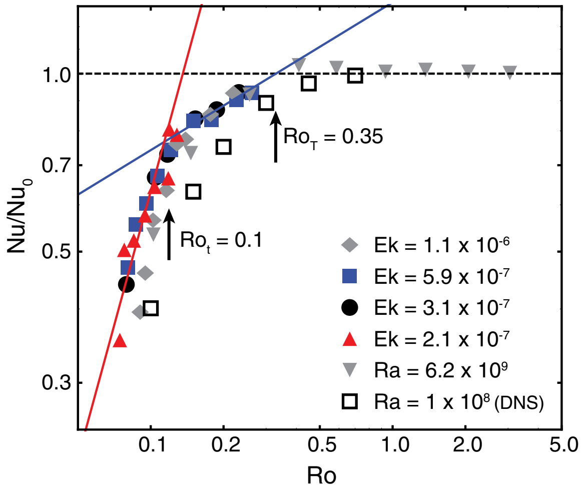

FIG. 2 (color online). Log-Log plot of $\mathrm{Nu}/\mathrm{Nu}_0$ vs Ro for constant Ek ($\mathrm{Nu}_0 = 0.121\mathrm{Ra}^{0.309}$): 1.1×10^{-6} (solid diamond, gray), 5.9×10^{-7} (solid square, blue), 3.1×10^{-7} (solid circle, black), 2.1×10^{-7} (solid up triangle, red), and for constant Ra: 6.2×10^9 (solid down triangle, gray), DNS [9]—1×10^8 (open square, black). The solid lines show approximate power law variations in the range $0.8 < \mathrm{Nu}/\mathrm{Nu}_0 < 1$ with $\mathrm{Nu}\sim\mathrm{Ra}^{0.45}$ (top, blue) and for $\mathrm{Nu}/\mathrm{Nu}_0 < 0.8$ with $\mathrm{Nu}\sim\mathrm{Ra}^{1.1}$—(bottom, red), respectively. Vertical arrows indicate approximate transition values.

for our data alone and $\beta = 1.65 \pm 0.1$ with the added constraint of the numerical data; both are consistent with $\beta = 7/4$, which is roughly an average of these two values. This is to be contrasted with the behavior for higher Pr

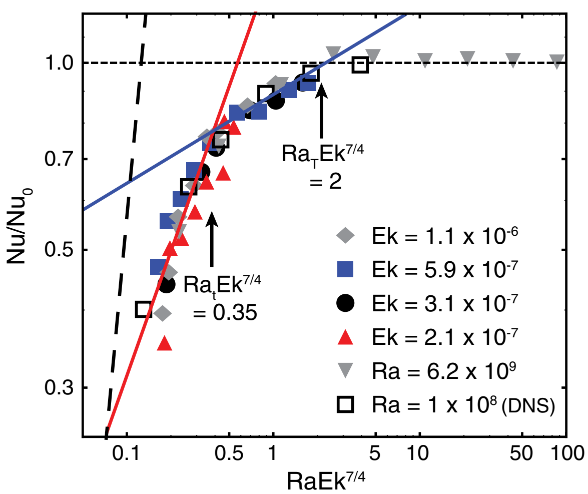

FIG. 3 (color online). Log-Log plot of $\mathrm{Nu}/\mathrm{Nu}_0$ vs $\mathrm{RaEk}^{7/4}$ for constant Ek: 1.1×10^{-6} (solid diamond, gray), 5.9×10^{-7} (solid square, blue), 3.1×10^{-7} (solid circle, black), 2.1×10^{-7} (solid up triangle, red), and for constant Ra: 6.2×10^9 (solid down triangle, gray), DNS [9]—1×10^8 (open square, black). The solid lines show approximate power law variations of the region $0.8<\mathrm{Nu}/\mathrm{Nu}_0<1$ with $(\mathrm{RaEk}^{7/4})^{1/7}$ (top, blue) and for $\mathrm{Nu}/\mathrm{Nu}_0<0.8$ with $(\mathrm{RaEk}^{7/4})^{2/3}$—$\mathrm{Nu}\sim\mathrm{Ra}$—(bottom, red), respectively. Vertical arrows indicates approximate transition values.

where recent analysis [24] suggested a dependence Ra $\mathrm{Ek}^{3/2}$ which is outside our experimental uncertainty. A composite fit for the high Pr data suggests $\mathrm{Ra}_t = 1.3\mathrm{Ek}^{-5/3}$ ($\beta = 1.67$). Our data suggest that the crossover dependence steepens slightly with decreasing Ek, with β varying from about 5/3 (1.67) to 1.8.

The power law straight lines in Fig. 3 are consistent with those in Fig. 2, yielding relationships of $\mathrm{Ra}^{0.45}$ and $\mathrm{Ra}^{1.0}$ for the Nu dependence on Ra. Again these lines are drawn for the purposes of describing the data collapse and are over quite limited ranges of parameters. There is no evidence for Ra^3 scaling as indicated by the dashed line in Fig. 3. Although we do not have an extended range for determining the dependence of Nu on Ra for $\mathrm{Ra} < \mathrm{Ra}_t$, one can infer that dependence by equating Nu dependences on Ra in the different regimes and knowing the measured dependence of Ra_t on Ek [8,22]. An advantage for our low Pr data is that the Nu is always large compared to 1 ($20 < \mathrm{Nu} < 440$) and the Ra dependence $\mathrm{Nu}_0(\mathrm{Ra})$ is well established over many decades [25,26]. Assuming power-law scaling in the geostrophic range of $\mathrm{Nu}\sim(\mathrm{Ra}/\mathrm{Ra}_c)^\gamma$, one has that $\gamma = 0.307\,3\beta/(3\beta-4)$ which yields $\gamma = 1.2$ for $\beta = 1.8$ and $\gamma = 1.6$ for $\beta = 1.65$. The theoretical/numerical prediction of the asymptotic scaling analysis [22], $\gamma = 1.5$, is included in this range.

A summary of the resultant phase diagram based on a combination of our measurements with measurements at larger Pr and Ek [8–10] (mostly water at different mean temperatures) is shown in Fig. 4 where we normalize Ra by the rotation-dependent linear stability value $\mathrm{Ra}_c = 7.8\mathrm{Ek}^{-4/3}$ [27]; presenting the data in this manner emphasizes the importance of achieving the condition $\mathrm{Ra}/\mathrm{Ra}_c \gg 1$ to achieve a strongly nonlinear turbulent state. The strong Pr dependence of the crossover from buoyancy-dominated to rotation-influenced thermal boundary layer turbulence is demonstrated by comparing lines A and B corresponding to lines of constant Ro of 2 and 0.35, respectively. Line C shows the extrapolation of our observed $\mathrm{Ra}_t \sim \mathrm{Ek}^{-1.8}$ dependence, whereas line D indicates $\mathrm{Ra}_t \sim \mathrm{Ek}^{-1.65}$. (The high Pr data for smaller Ek [11] show an abrupt increase at $\mathrm{Ek} \approx 5\times10^{-6}$, an apparently unnoticed and unexplained feature of the high Pr data). The upper limit of self-consistency for arguments [24,28] leading to $\mathrm{Nu}\sim\mathrm{Ra}^3\mathrm{Ek}^4$ corresponds to $\mathrm{Ra}/\mathrm{Ra}_c \lesssim \mathrm{Ek}^{-1/6}$ and implies little accessible range of such scaling in the available parameter space.

Expanding on the limits for a geostrophic turbulence regime, numerical simulations [22] suggest that one needs $\mathrm{Ra}/\mathrm{Ra}_c$ to be larger than about 4 to enter a regime of geostrophic turbulence. We denote this limit in Fig. 4 as line D with a generous $\mathrm{Ra}/\mathrm{Ra}_c = 3$. One implication of this cutoff that can be drawn from the phase diagram is that experiments at larger $\mathrm{Ek} > 10^{-5}$ cannot have a measurable range of geostrophic turbulence. In principle, one would like measurements of Nu over a range of Ra such that

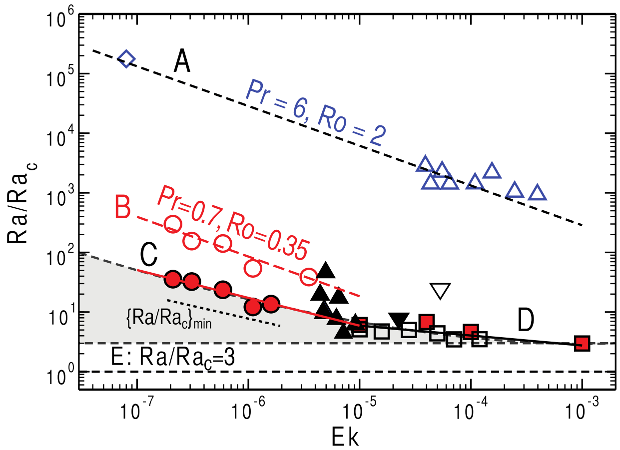

FIG. 4 (color online). Phase diagram of rotating convection in parameters $\mathrm{Ra}/\mathrm{Ra}_c$ and Ek. Rotation first affects turbulent convection below line A for $\mathrm{Pr} = 6$ ($\mathrm{Ro}_T = 2$) and below line B for $\mathrm{Pr} = 0.7$ ($\mathrm{Ro}_T = 0.35$). The crossover to geostrophic turbulence for $\mathrm{Pr} = 0.7$ occurs along line C where $\mathrm{Ra}_t = 0.25\mathrm{Ek}^{-1.8}$ (the dotted line below C is the lower limit of data presented here) whereas line D describes the higher Pr data with $\mathrm{Ra}_t = 1.3\mathrm{Ek}^{-1.65}$. Line E indicates $\mathrm{Ra}/\mathrm{Ra}_c = 3$ which is the rough upper bound to a regime of weakly nonlinear convection near onset ($\mathrm{Ra}/\mathrm{Ra}_c = 1$). Data are from Ref. [8] (solid square—red), Refs. [9,11] [open (blue) and solid (black) up triangles], Ref. [10] (solid down triangles, black), Ref. [25] (open diamond, blue), and this Letter (open and solid circles, red). The shaded region corresponds to states where geostrophic turbulence may be accessible.

$\mathrm{Ra}_c \ll \mathrm{Ra} \ll \mathrm{Ra}_t$. This limit suggests that one needs $\mathrm{Ek} < 10^{-7}$ to achieve a sufficient range to measure a decade of scaling of Nu with Ra in the geostrophic turbulence range and $\mathrm{Ek} < 10^{-9}$ to approach two decades. This will be a stiff challenge for future experiments. In the present case, it is unclear whether our scaling of $\mathrm{Nu} \sim (\mathrm{Ra}/\mathrm{Ra}_c)^\gamma$ with $\gamma \approx 1$ is obtained far enough below Ra_t not to be influenced by that crossover; i.e., larger values of γ are not ruled out by our measurements. Nevertheless, the data presented here have the lowest Ek (highest dimensionless rotation rate) and largest range that resolves the geostrophic turbulence range of experiments performed until now.

Measurements for large Pr indicated that the aspect ratio Γ plays a role in determining Ra_T [12] and that there is a Pr dependence of the crossover to rotation-influenced turbulent convection [11] of approximately $\mathrm{Ro}_T \sim \mathrm{Pr}^{0.4}$. On the first point, the data at very high Ra in helium gas with $\Gamma = 0.5$ [25] suggest that the transition remains at $\mathrm{Ro}_T \approx 2$ independent of Γ so there may be Ra dependence since an implication of the measured Γ dependence [12] would be $\mathrm{Ro}_T \approx 4$. Second, if we take lines A and B as describing the data for $\mathrm{Pr} = 6$ and $\mathrm{Pr} = 0.7$, respectively, the implied Pr dependence would be $\mathrm{Ro}_T \sim \mathrm{Pr}^{0.8}$ rather than the previously indicated $\mathrm{Pr}^{0.4}$ dependence [11]. Finally, if a Ra^3 range were to exist it would only be self-consistent if the assumed boundary layer stability was the same as the bulk [24] which translates to the condition $\mathrm{Ra}/\mathrm{Ra}_c \lesssim \mathrm{Ek}^{-1/6}$ (corresponding to $\mathrm{Ra}_c^\delta \gtrsim 1000$ where δ is the boundary layer thickness). Even at $\mathrm{Ek} = 10^{-8}$, below even the data presented here, the criterion for a possible Ra^3 regime would be $\mathrm{Ra}/\mathrm{Ra}_c < 20$. Based on this estimate, it seems unlikely that one could observe this regime for $\mathrm{Ek} > 10^{-5}$, with a solid decade of scaling only possible for $\mathrm{Ek} < 10^{-9}$.

The phase diagram in Fig. 4 suggests the following: (1) The transition from buoyancy dominated turbulent convection to rotation influenced turbulent convection depends sensitively on Pr and approximately linearly on Ro; (2) The transition from rotation-influenced to rotation-dominated convection is best described by a transition relationship $\mathrm{Ra}_t \sim \mathrm{Ek}^{-\beta}$ with little or no Pr dependence in the overall amplitude but a possible increase in β in the range $1.65 < \beta < 1.8$ for lower Pr and/or smaller Ek; (3) For $\mathrm{Ek} > 10^{-5}$, which includes almost all of the data taken for water with $\mathrm{Pr} \approx 5$ [5–10], the available range of $\mathrm{Ra}/\mathrm{Ra}_c$ is insufficient to observe geostrophic turbulence scaling [22] or $\mathrm{Ra}^3\mathrm{Ek}^4$ scaling [24]; (4) Direct measurement of the dependence $\mathrm{Nu} \sim (\mathrm{Ra}/\mathrm{Ra}_c)^\gamma$ indicates $\gamma \approx 1$ whereas values inferred from the crossover condition at $\mathrm{Ra}_t(\mathrm{Ek})$ yield $1.2 < \gamma < 1.6$. There are thus many experimental and numerical challenges (recent numerical work on rotating convection is approaching the values shown here with comparable results [29]) that need to be addressed to further characterize and extend the fascinating problem of rotating thermal convection to geophysically relevant ranges of parameters.

We acknowledge important conversations with K. Julien, A. Rubio, and G. Vasil concerning predictions of numerical simulations and G. Ahlers for helpful comments. Contributions by R. E. were funded by the National Nuclear Security Administration of the U.S. Department of Energy at Los Alamos National Laboratory under Contract No. DE-AC52-06NA25396. We acknowledge the Elettra Synchrotron Light Laboratory, Trieste, for providing technical and logistical assistance and, in particular, we wish to thank Mr. P. Tosolini.

*Corresponding author.
ecke@lanl.gov

[1] G. Glatzmaier, R. Coe, L. Hongre, and P. Roberts, Nature (London) **401**, 885 (1999).
[2] J. Marshall and F. Schott, Rev. Geophys. **37**, 1 (1999).
[3] M. Heimpel, J. Aurnou, and J. Wicht, Nature (London) **438**, 193 (2005).
[4] E. A. Spiegel, Annu. Rev. Astron. Astrophys. **9**, 323 (1971).
[5] H. T. Rossby, J. Fluid Mech. **36**, 309 (1969).
[6] F. Zhong, R. E. Ecke, and V. Steinberg, J. Fluid Mech. **249**, 135 (1993).
[7] Y. Liu and R. E. Ecke, Phys. Rev. Lett. **79**, 2257 (1997).
[8] E. King, S. Stellmach, J. Noir, U. Hansen, and J. Aurnou, Nature (London) **457**, 301 (2009).

[9] J. Q. Zhong, R. J. A. M. Stevens, H. J. H. Clercx, R. Verzicco, D. Lohse, and G. Ahlers, Phys. Rev. Lett. **102**, 044502 (2009).
[10] Y. Liu and R. E. Ecke, Phys. Rev. E **80**, 036314 (2009).
[11] J. Q. Zhong and G. Ahlers, J. Fluid Mech. **665**, 300 (2010).
[12] S. Weiss and G. Ahlers, J. Fluid Mech. **684**, 407 (2011).
[13] S. Weiss and G. Ahlers, J. Fluid Mech. **688**, 461 (2011).
[14] S. Chandrasekhar, *Hydrodynamic and Hydromagnetic Stability* (Oxford University Press, Oxford, 1961).
[15] P. P. Niiler and F. E. Bisshopp, J. Fluid Mech. **22**, 753 (1965).
[16] K. Julien, S. Legg, J. McWilliams, and J. Werne, J. Fluid Mech. **322**, 243 (1996).
[17] M. Sprague, K. Julien, E. Knobloch, and J. Werne, J. Fluid Mech. **551**, 141 (2006).
[18] R. J. A. M. Stevens, J. Q. Zhong, H. J. H. Clercx, G. Ahlers, and D. Lohse, Phys. Rev. Lett. **103**, 024503 (2009).
[19] J. M. Pfotenhauer, J. J. Niemela, and R. J. Donnelly, J. Fluid Mech. **175**, 85 (1987).
[20] F. Zhong, R. E. Ecke, and V. Steinberg, Phys. Rev. Lett. **67**, 2473 (1991).
[21] I. Grooms, K. Julien, J. B. Weiss, and E. Knobloch, Phys. Rev. Lett. **104**, 224501 (2010).
[22] K. Julien, E. Knobloch, A. M. Rubio, and G. M. Vasil, Phys. Rev. Lett. **109**, 254503 (2012).
[23] B. M. Boubnov and G. S. Golitsyn, J. Fluid Mech. **219**, 215 (1990).
[24] E. King, S. Stellmach, and J. Aurnou, J. Fluid Mech. **691**, 568 (2012).
[25] J. J. Niemela, S. Babuin, and K. R. Sreenivasan, J. Fluid Mech. **649**, 509 (2010).
[26] J. J. Niemela, L. Skrbek, K. R. Sreenivasan, and R. J. Donnelly, Nature (London) **404**, 837 (2000).
[27] Per Ref. [15], the coefficient A in $\mathrm{Ra}_c = AE_k^{-4/3}$ depends weakly on E_k with values between 7.5 and 8.1 over the range of E_k in the experiment (the asymptotic value is 8.7). We take $A = 7.8$ to compute Ra_c.
[28] B. M. Boubnov and G. S. Golitsyn, J. Fluid Mech. **167**, 503 (1986).
[29] S. Horn and S. Shishkina, arXiv:1404.7755.